Gas-Phase Acidities of Cysteine-Polyalanine Peptides I: $A_{3,4}CSH$ and $HSCA_{3,4}$

Jianhua Ren,*,† John P. Tan,‡ and Robert T. Harper§

Department of Chemistry, University of the Pacific, Stockton, California 95211

Received: April 19, 2009; Revised Manuscript Received: August 18, 2009

The gas-phase acidities of four cysteine-polyalanine peptides, $A_{3,4}CSH$ and $HSCA_{3,4}$, were determined using the extended Cooks kinetic method with full entropy analysis. A triple-quadrupole mass spectrometer with an electrospray interface was employed for the experimental study. The ion activation was achieved via collision-induced dissociation (CID) experiments. The deprotonation enthalpies ($\Delta_{acid}H$) of the peptides were determined to be 332.2 ± 2.0 kcal/mol (A_3CSH), 325.9 ± 2.0 kcal/mol (A_4CSH), 319.3 ± 3.0 kcal/mol ($HSCA_3$), and 319.2 ± 4.0 kcal/mol ($HSCA_4$). The deprotonation entropies ($\Delta_{acid}S$) of the peptides were estimated based on the entropy term ($\Delta(\Delta S)$) and the deprotonation entropies of the reference acids. By using the deprotonation enthalpies and entropies, the gas-phase acidities ($\Delta_{acid}G$) of the peptides were derived: 325.0 ± 2.0 kcal/mol (A_3CSH), 320.2 ± 2.0 kcal/mol (A_4CSH), 316.3 ± 3.0 kcal/mol ($HSCA_3$), and 315.4 ± 4.0 kcal/mol ($HSCA_4$). Conformations and energetic information of the peptides were calculated through simulated annealing (Tripos), geometry optimization (AM1), and single-point energy calculations (B3LYP/6-31+G(d)), respectively. The calculated theoretical deprotonation enthalpies ($\Delta_{acid}H$) of 334.2 kcal/mol (A_3CSH), 327.7 kcal/mol (A_4CSH), 320.6 kcal/mol ($HSCA_3$), and 318.6 kcal/mol ($HSCA_4$) are in good agreement with the experimentally determined values. Both the experimental and computational studies suggest that the two N-terminal cysteine peptides, $HSCA_{3,4}$, are significantly more acidic than the corresponding C-terminal ones, $A_{3,4}CSH$. The high acidities of the former are likely due to the helical conformational effects for which the thiolate anion may be strongly stabilized by the interaction with the helix macrodipole.

Introduction

The acidities of amino acid residues are among the most important thermochemical properties that influence the structures, the reactivity, and the folding−unfolding processes of proteins.[1,2] Individual amino acid residues often exhibit different acidities depending on their location in proteins. In particular, the residue located at or near the N-terminus of a helix is often more acidic than that at or near the C-terminus.[3,4] An example is the cysteine residue residing in the active sites of the thioredoxin superfamily of enzymes.[5,6] This family of enzymes catalyzes the reduction of the disulfide bonds in proteins.[7] The active site of the enzymes has a helix loop, and the cysteine residue (the thiol group, SH) located at the N-terminus of the helix is extremely acidic with pK_a values ranging from 3.5 to 6.7, significantly lower than those in unfolded proteins or an isolated cysteine (pK_a ∼ 8.5).[8−10] One possible factor causing the unusual acidity of the N-terminal cysteine may come from the interaction of the ionized cysteine (the thiolate anion) with the helix macrodipole.[11−13] There have been extensive experimental studies on the acid−base properties of helical peptides reported in the literature. However, these studies were all carried out in aqueous solutions.[4,14−16] The results were often complicated by solvent effects.[15] In fact, most of the active sites in proteins are located near the interior region where solvent effects are minimized.[1,17] For these reasons, studies of the conformational effects on acid−base properties of peptides in a solvent-free environment are of great importance.

The acidities of amino acid residues also play important roles in the gas-phase ion chemistry of peptides and proteins, including the ion intensities of negative ions in different ionization processes, the fragmentation mechanisms under tandem mass spectrometry (MS/MS) conditions, and hydrogen/deuterium exchange patterns. A recent study shows that the ion intensities of the negative ions of amino acids and peptides from fast atom bombardment (FAB), matrix-assisted laser desorption ionization (MALDI), and electrospray ionization (ESI) are tightly correlated to the gas-phase acidities.[18] Extensive investigations of peptide fragmentation mechanisms suggest that protonated peptides preferentially cleave at the peptide bond C-terminal to acidic residues.[19−23] Similarly, acidic residues often have strong effects on the fragmentation pathways of negatively charged peptides. Favored cleavages often occur at the peptide bond adjacent to acidic residues.[24−27] Interestingly, sodiumated or copperated peptides also exhibit selective cleavage adjacent to acidic residues.[28,29] In addition, the presence of strongly acidic amino acid residues has a dramatic impact on the observed hydrogen/deuterium exchange patterns of charged gas-phase peptides and proteins, presumably due to conformation changes.[30,31]

Despite the importance of the acidic amino acid residues in peptides and proteins, knowledge of the quantitative information of the gas-phase acidities of amino acid residues is very limited. The gas-phase acidities of isolated amino acids and simple derivatives have been determined experimentally using different gas-phase techniques.[32−40] Recent studies provided conflicting results regarding the relative acidities of the two acidic groups in cysteine. Results from photoelectron spectroscopy and gas-phase hydrogen−deuterium exchange experiments show that the thiol group (SH) is more acidic than the carboxyl group (CO_2H).[36,41] On the other hand, gas-phase infrared multiple

* Corresponding author. E-mail: jren@pacific.edu. Phone: 209-946-2393. Fax: 209-946-2607.
† University of the Pacific.
‡ University of California, Los Angeles, Dental School Graduate Program.
§ Lincoln High School, Stockton, California.

10.1021/jp903594a CCC: $40.75
Published on Web 09/15/2009

photon dissociation (IRMPD) experiment suggest that the deprotonation site is the carboxyl group and not the thiol group.[42] For peptides, only a few apparent acidities had been examined to date.[43]

In connection with the investigations of the conformational effects on the gas-phase acidities of peptides, we have studied a series of cysteine-polyalanine peptides via mass spectrometry measurements and computational studies. We have previously reported the determination of the gas-phase acidities of two oligo-cysteine-polyalanine peptides, Cys-$(Ala)_{3,4}$ ($HSCA_{3,4}$).[44] Due to scattered data points in some experiments, we assigned a relatively large uncertainty. For this study, we remeasured the acidities of these two peptides by extending the number of repeating measurements and an improved data analysis procedure. In addition, we performed computational studies by modeling the conformations of the neutral and the ionized peptides and by calculating the theoretical acidities. To examine the peptide sequence effect on the observed acidity, we also studied two C-terminal cysteine analogues, $(Ala)_{3,4}$-Cys ($A_{3,4}CSH$), using similar procedures. In all these peptides, the C-termini are amidated to avoid the complication by the C-terminal carboxyl group. The acidities are referred to those of the thiol group (SH) of the cysteine residue. In this paper, we report the studies of these four peptides both experimentally and computationally.

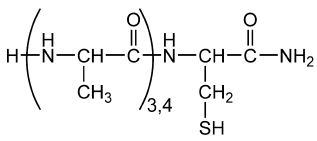

$A_{3,4}CSH$

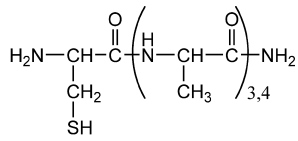

$HSCA_{3,4}$

Experimental Methods

The gas-phase acidity of an acid (AH), $\Delta_{acid}G(AH)$, is defined as the Gibbs free energy change of the deprotonation reaction (generally at 298 K), $AH \rightarrow A^- + H^+$. The deprotonation entyalpy of AH, $\Delta_{acid}H(AH)$, is the enthalpy change of the same deprotonation reaction. The deprotonation entropy of AH is the entropy change of the reaction, $\Delta_{acid}S(AH) = S(A^-) + S(H^+) - S(AH)$, where $S(H^+)$ is 26 cal/mol K (at 298 K).[45]

Mass Spectrometry Measurements. The deprotonation enthalpies ($\Delta_{acid}H$) of the peptides A_nCSH and $HSCA_n$, where $n = 3$ and 4, were determined by using the extended Cooks kinetic method in which entropy effects were taken into consideration.[46−50] The validity and limitations of using the extended Cooks kinetic method to determine thermochemical quantities have been thoroughly discussed in the literature.[51−57] Because of the nonvolatile and thermally labile nature of peptides, the kinetic method is the most practical approach available at present to produce reasonably accurate acid−base thermochemical quantities of peptides.[58] The general procedure can briefly be described as following. A series of proton-bound heterodimers ($[A\cdot H\cdot A_i]^-$) of deprotonated peptides, A^- ($^-SCA_n$ or A_nCS^-), with a set of conjugate bases of reference acids (HA_i) were generated in the electrospray ionization (ESI) source of the mass spectrometer. The reference acids all have known gas-phase acidities. Each proton-bound dimer was activated by collisions with argon atoms and underwent competitive unimolecular dissociations (the CID process) to produce two ionic products, A^- and A_i^-, with rate constants of k and k_i, respectively (Scheme 1).

SCHEME 1

$$AH + A_i^- \underset{}{\overset{k_i}{\leftarrow}} [A\bullet H\bullet A_i]^- \xrightarrow{k} A^- + HA_i$$

It is assumed that there are no reverse activation barriers for either dissociation channel, and the natural logarithm of the ratio of the rate constants has a linear correlation to the difference in the gas-phase acidities, eq 1, where R is the universal gas constant; T_{eff} is called the "effective temperature"; $\Delta_{acid}G$ and $\Delta_{acid}G_i$ are the gas-phase acidities of HA and the reference acid (HA_i); and $\Delta_{acid}H$ and $\Delta_{acid}H_i$ are the corresponding deprotonation enthalpies. The effective temperature is an empirical parameter (or a kinetic correlation parameter) that depends on several experimental variables and properties of the proton-bound dimers.[59−64] The term $\Delta(\Delta S)$ is the difference of the activation entropies between the two competing dissociation channels, $\Delta(\Delta S) = \Delta S^{\ddagger}$(with k) $- \Delta S^{\ddagger}$(with k_i). If the reference acids all have similar structures, then the term $\Delta(\Delta S)$ can be assumed to be constant. Under the assumption of the negligible reverse activation barrier, $\Delta(\Delta S)$ can be calculated using the deprotonation entropies of the two acids (HA and HA_i), $\Delta(\Delta S) \approx \Delta_{acid}S - \Delta_{acid}S_i$. The ratio of the rate constants (k/k_i) can be replaced by the CID product ion branching ratios ($[A^-]/[A_i^-]$), if the secondary fragmentation is negligible.

To obtain the value of $\Delta_{acid}H$, the proton-bound dimers were activated at several different collision energies, and the CID product ion branching ratios were measured at each of the collision energies. Two sets of thermokinetic plots would be generated. The first set consists of linear plots of $\ln([A^-]/[A_i^-])$ versus $\Delta_{acid}H_i$ with $1/RT_{eff}$ as the slope and $-[\Delta_{acid}H/RT_{eff} - \Delta(\Delta S)/R]$ as the intercept. Ideally, all plots cross at a single point at which $\Delta_{acid}H = \Delta_{acid}H_i$ and $\ln([A^-]/[A_i^-]) = \Delta(\Delta S)/R$. This crossing point is referred to as the isothermal point or isoequilibrium point.[52,55] The value of $\Delta_{acid}H$ corresponding to the isothermal point is obtained from the second set of the thermokinetic plots. The plot of $[(\Delta_{acid}H/RT_{eff} - \Delta(\Delta S)/R]$ obtained from the first set against $1/RT_{eff}$ generates a Van't Hoff-like plot with a slope of $\Delta_{acid}H$ and an intercept of $-\Delta(\Delta S)/R$. To have a proper statistical treatment of the uncertainty throughout the data analysis, the average deprotonation enthalpy of the reference acids, $\Delta_{acid}H_{avg}$, was introduced, and eq 1 was converted to eq 2, where $\ln([A^-]/[A_i^-])$ has a linear relationship with $\Delta_{acid}H_i - \Delta_{acid}H_{avg}$.[65] The first set of plots would be $\ln([A^-]/[A_i^-])$ versus $\Delta_{acid}H_i - \Delta_{acid}H_{avg}$ with $1/RT_{eff}$ as the slope and $-[(\Delta_{acid}H - \Delta_{acid}H_{avg})/RT_{eff} - \Delta(\Delta S)/R]$ as the intercept. The second linear plot would be $[(\Delta_{acid}H - \Delta_{acid}H_{avg})/RT_{eff} - \Delta(\Delta S)/R]$ against $1/RT_{eff}$ with a slope of $\Delta_{acid}H - \Delta_{acid}H_{avg}$ and an intercept of $-\Delta(\Delta S)/R$. The deprotonation entropy of HA, $\Delta_{acid}S$, can be calculated using the equation $\Delta_{acid}S = \Delta(\Delta S) + \Delta_{acid}S_i$. Since $\Delta_{acid}S_i$ slightly varies from one reference acid to the other, the averaged value of $\Delta_{acid}S_i$ will be used in this work. By combining $\Delta_{acid}H$ and the entropy term, $T(\Delta_{acid}S)$, the gas-phase acidity of the acid HA, $\Delta_{acid}G$, can be derived using eq 3, where $T = 298$ K.

$$\ln\left(\frac{k}{k_i}\right) = \frac{\Delta_{acid}G_i - \Delta_{acid}G}{RT_{eff}} = \frac{\Delta_{acid}H_i - \Delta_{acid}H}{RT_{eff}} + \frac{\Delta(\Delta S)}{R} \text{ where } \frac{k}{k_i} \approx \frac{[A^-]}{[A_i^-]} \text{ and } \Delta(\Delta S) \approx \Delta_{acid}S - \Delta_{acid}S_i \quad (1)$$

$$\ln\frac{[A^-]}{[A_i^-]} = \frac{\Delta_{acid}H_i - \Delta_{acid}H_{avg}}{RT_{eff}} - \left[\frac{\Delta_{acid}H - \Delta_{acid}H_{avg}}{RT_{eff}} - \frac{\Delta(\Delta S)}{R}\right] \quad (2)$$

$$\Delta_{acid}G = \Delta_{acid}H - T(\Delta_{acid}S) \quad (3)$$

The uncertainty of the average acidity ($\Delta_{acid}H_{avg}$) was calculated as the root sum square of the random and systematic errors. For example, for the A_3CSH system, the random error was treated as the averaged uncertainty of the reference acids (±2.2 kcal/mol) divided by the square root of the number of the reference acids, $(2.2/\sqrt{6}) = 0.9$ kcal/mol, and the systematic error was assigned as $\sqrt{2.2} = 1.5$ kcal/mol. The root sum square of the random and systematic errors yielded $\sqrt{(0.9^2 + 1.5^2)} = 1.7$ kcal/mol. The uncertainty of the data resulting from the linear regression was estimated by weighted orthogonal distance regression (ODR) using the ODRPACK suite of programs.[66] In addition, the ODRFIT program developed by Ervin and Armentrout was also used to analyze the uncertainty.[52] This program incorporates the ODRPACK and Monte Carlo simulations for error analysis where random errors (measurement error and error in reference acidities) are treated as Gaussian distributions with ± two standard deviations (95% confidence limit). By fitting experimental data, it forces all lines to intersect at a single point. In this work, we used a standard deviation of 4 kJ/mol (~1 kcal/mol) for the reference and 0.049 for $\ln([A^-]/[A_i^-])$, and these correspond to ±8 kJ/mol (~2 kcal/mol) and ±10%, respectively. We set 5000 iterations in the Monte Carlo simulations.

The experiments were carried out using a triple quadrupole mass spectrometer (Varian 1200 L, Varian Inc., Walnut Creek, CA) located in the Mass Spectrometry Center of the Chemistry Department at the University of the Pacific. The instrument consists of a near-horizontal ESI source with nitrogen drying gas flowing through a capillary, a hexapole ion guide at a pressure of about 1 mTorr, and a triple quadrupole mass analyzer with a curved collision chamber. Ions generated in the ESI source are presumed to be thermalized by multiple collisions with the bath gas molecules in the ion guide chamber. The voltage of the ESI needle was set at −4.5 kV, and the drying gas temperature was set at 150 °C. The first important step to carry out the acidity measurements was to generate stable proton-bound heterodimer ions. The dimer ions were formed by syringe infusion of a solution of methanol and water (50/50, v/v) containing a mixture of a reference acid and a peptide ($10^{-5}-10^{-4}$ M) into the ESI (negative mode) chamber at a flow rate of 10 μL/min. The signal of the dimer ion was optimized by adjusting the instrumental conditions, especially the capillary voltage. The dimer ion was isolated by the first quadrupole and subsequently subjected to CID experiments in the collision chamber with argon as the collision gas. The dissociation product ions were analyzed by the third quadrupole. To determine the CID product ion ratios, the CID product ion intensities were measured by setting the instrument in the single reaction monitoring (SRM) mode (centroid) in which the scan was focused on selected product ions. For each proton-bound heterodimer, the CID experiment was carried out at several collision energies between 0.5 and 2.5 eV in the center-of-mass frame (E_{cm}). At too low a collision energy, the minor CID product ions' signals were unstable, and at too high a collision energy, secondary fragmentations were significant. The center-of-mass energy was calculated using the following equation: $E_{cm} = E_{lab}[m/(M + m)]$, where E_{lab} is the collision energy in laboratory frame; m is the mass of argon; and M is the mass of the proton-bound dimer ion. Multiple measurements were performed on different days, and the CID product ion ratios were reproducible with a relative uncertainty within ±5%.

Several nonideal conditions were examined. The possible secondary fragmentations were examined by recording the CID spectra at several collision energies for each proton-bound heterodimer with a wider range of the m/z window. The observed secondary fragments were taken into consideration for the data analysis. The collision gas effects on the CID product ion ratios were evaluated by performing the CID experiments at several collision gas pressures, ranging from 0.40 to 0.70 mTorr (software readout). At too low a pressure, the minor CID product ion intensities were unstable, and at too high a pressure, multiple secondary fragmentations became significant when the collision energy was increased. In this paper, the data were measured at the collision gas pressure of 0.50 ± 0.03 mTorr.

The peptides were synthesized in our laboratory using the standard method of solid phase peptide synthesis.[67−69] The apparatus consists of a glass peptide synthesis vessel (Kemtech America, Inc., Whittier, CA) mounted on an agitator assembled in our laboratory. The aminomethyl Rink amide resin (Sigma-Aldrich Co., Milwaukee, WI) was used as the solid support to yield the peptides with amide C-termini. All chemicals used in the peptide synthesis, including fmoc−cysteine and fmoc−alanine, were purchased from Sigma-Aldrich Chemical Co. and were used without further purification.

Computational Methods. The conformations of the neutral and deprotonated peptides were calculated by the simulated annealing process using the Tripos force field implemented in the SYBYL 7.2 package of programs (Tripos, Inc., St. Louis, MO). The peptide starting structures were ideal α-helices. The general procedure involved heating the system to 500 K for 1500 fs, followed by annealing to 50 K for 1500 fs for 100 cycles per simulation. Structures were saved at regular intervals (50 fs) throughout the simulations. Upon completion, the ten lowest-energy conformations for each peptide were selected for further geometry optimization using the AM1 semiempirical method[70] implemented in the Gaussian W03 suite of programs.[71] Vibrational frequencies were also calculated using AM1 to yield the zero-point energies and the thermal corrections to the enthalpy at 298 K. True energy minima were determined by checking the absence of imaginary frequencies from the set of obtained frequencies. Following geometry optimization, single point energies were calculated using density functional theory at the B3LYP/6-31+G(d) level.[72−75] The enthalpy for each species was obtained by combining the electronic energy calculated at the B3LYP level and the zero-point energy plus

TABLE 1: Thermochemical Quantities of the Reference Acids Used in This Research

reference acid[a]	$\Delta_{acid}H$, expt[b] (kcal/mol)	$\Delta_{acid}G$, expt[b] (kcal/mol)	$\Delta_{acid}S$[c] (cal/mol K)
$ClCH_2CO_2H$ (MCAH)	336.5 ± 2.2	329.0 ± 2.0	25.2
$BrCH_2CO_2H$ (MBAH)	334.8 ± 2.3	328.2 ± 2.0	22.1
F_2CHCO_2H (DFAH)	331.0 ± 2.2	323.8 ± 2.0	24.2
Cl_2CHCO_2H (DCAH)	328.4 ± 2.1	321.9 ± 2.0	21.8
Br_2CHCO_2H (DBAH)	328.3 ± 2.2	321.3 ± 2.0	23.5
F_3CCO_2H (TFAH)	323.8 ± 2.9	317.4 ± 2.0	21.5
$C_3F_7CO_2H$ (HFAH)	321.9 ± 2.2	314.9 ± 2.0	23.5

[a] The names (e.g., MCAH) are the abbreviations used in this paper. [b] Obtained from the NIST Chemistry Webbook.[45] [c] Derived from the relationship $\Delta G = \Delta H - T(\Delta S)$, where $T = 298$ K. It is assumed that each $\Delta_{acid}S$ value has 2.0 cal/mol K uncertainty.

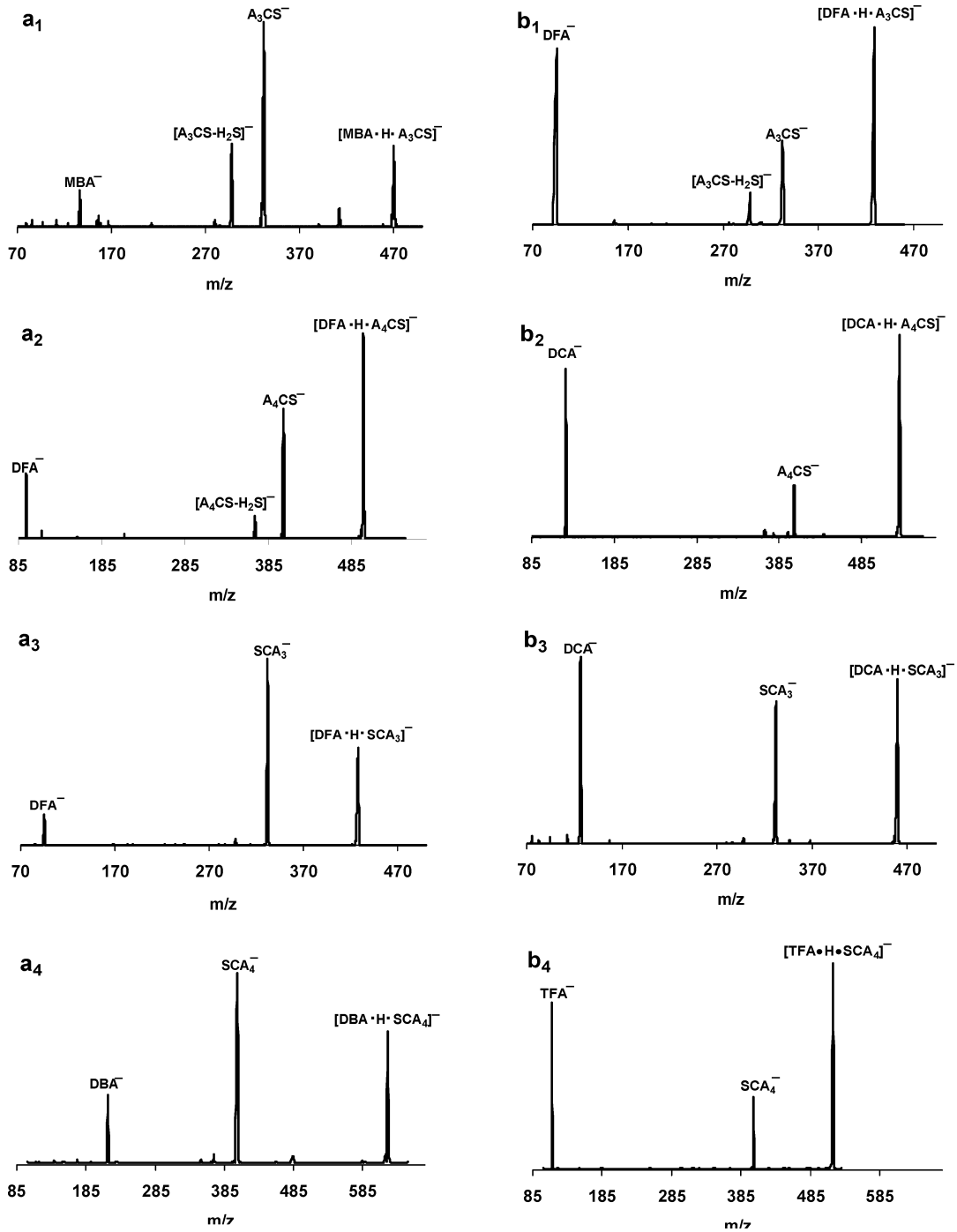

Figure 1. CID spectra collected at 1.5 eV (E_{cm}) collision energy for $[MBA\cdot H\cdot A_3CS]^-$ (a_1), $[DFA\cdot H\cdot A_3CS]^-$ (b_1), $[DFA\cdot H\cdot A_4CS]^-$ (a_2), $[DCA\cdot H\cdot A_4CS]^-$ (b_2), $[DFA\cdot H\cdot SCA_3]^-$ (a_3), $[DCA\cdot H\cdot SCA_3]^-$ (b_3), $[DBA\cdot H\cdot SCA_4]^-$ (a_4), and $[TFA\cdot H\cdot SCA_4]^-$ (b_4).

the thermal correction calculated using the AM1 method. The theoretically predicted deprotonation enthalpy for each peptide was calculated using an isodesmic proton transfer reaction with ethane thiol (CH_3CH_2SH) as the reference acid (eq 4).

$$A_nCSH + CH_3CH_2S^- \rightarrow A_nCS^- + CH_3CH_2SH \quad (4)$$

Results of Experimental Studies

The relative acidities of the peptides were first bracketed against a series of known reference acids by using standard full product ion scan CID experiments. Seven structurally similar halogenated carboxylic acids were selected as the references: $ClCH_2CO_2H$ (MCAH), $BrCH_2CO_2H$ (MBAH), F_2CHCO_2H (DFAH), Cl_2CHCO_2H (DCAH), Br_2CHCO_2H (DBAH), F_3CCO_2H (TFAH), and $CF_3CF_2CF_2CO_2H$ ($C_3F_7CO_2H$) (HFAH). The gas-phase acidities and related thermochemical properties of these molecules are listed in Table 1. The CID experiments were performed with the proton-bound heterodimer ions, $[A_i\cdot H\cdot A_{3,4}CS]^-$ and $[A_i\cdot H\cdot SCA_{3,4}]^-$, at 1.5 eV ($E_{cm}$) collision energy under 0.5 mTorr of argon gas. The relative acidity of each peptide can be examined by comparing the relative intensities of the CID product ions. If the peptide is a stronger acid than the corresponding reference acid, then the CID product ion intensity of the deprotonated peptide will be stronger than that of the deprotonated reference acid. Selected CID spectra

TABLE 2: Values of the Natural Logarithms of the CID Product Ion Ratios (a) ln([$A_{3,4}CS^-$]/[A_i^-]), from the Dissociation of [$A_{3,4}CS\cdot H\cdot A_i]^-$, and (b) ln([$SCA_{3,4}^-$]/[$A_i^-$]), from the Dissociation of [$SCA_{3,4}\cdot H\cdot A_i]^-$, at Four Collision Energies, E_{cm} (with ±5% of Uncertainty) under 0.5 mTorr of Collision Gas Pressure

	(a) A_3CSH				A_4CSH			
	$\Delta_{acid}H_{avg}$ = 330.5 kcal/mol[a]				$\Delta_{acid}H_{avg}$ = 327.4 kcal/mol[a]			
	$\Delta_{acid}S_{avg}$ = 23.0 cal/mol K[b]				$\Delta_{acid}S_{avg}$ = 23.2 cal/mol K[b]			
HA_i	1.0 eV	1.5 eV	2.0 eV	2.5 eV	1.0 eV	1.5 eV	2.0 eV	2.5 eV
$ClCH_2CO_2H$	3.68	3.50	3.39	3.45				
$BrCH_2CO_2H$	2.83	2.65	2.45	2.24				
F_2CHCO_2H	−0.442	−0.268	−0.0921	0.167	1.04	1.25	1.87	2.34
Cl_2CHCO_2H	−2.60	−2.41	−2.22	−2.13	−0.901	−0.803	−0.692	−0.598
Br_2CHCO_2H	−2.43	−2.44	−2.49	−2.60	−1.02	−1.11	−1.24	−1.40
F_3CCO_2H	−5.41	−5.02	−4.71	−4.44				
$C_3F_7CO_2H$					−4.22	−4.30	−4.50	−4.58
	(b) $HSCA_3$				$HSCA_4$			
	$\Delta_{acid}H_{avg}$ = 326.7 kcal/mol[a]				$\Delta_{acid}H_{avg}$ = 325.6 kcal/mol[a]			
	$\Delta_{acid}S_{avg}$ = 22.9 cal/mol K[b]				$\Delta_{acid}S_{avg}$ = 22.6 cal/mol K[b]			
HA_i	1.0 eV	1.5 eV	2.0 eV	2.5 eV	1.0 eV	1.5 eV	2.0 eV	2.5 eV
F_2CHCO_2H	2.54	1.92	1.64	1.61				
Cl_2CHCO_2H	0.216	−0.207	−0.463	−0.580	2.09	1.50	1.19	1.06
Br_2CHCO_2H	−0.0740	−0.465	−0.753	−0.976	1.57	1.02	0.602	0.327
F_3CCO_2H	−2.69	−2.94	−2.99	−3.00	−0.889	−1.14	−1.19	−1.03
$C_3F_7CO_2H$	−4.80	−4.96	−5.02	−5.06	−3.35	−3.56	−3.71	−3.85

[a] Average deprotonation enthalpy of the set of selected reference acids. [b] Average deprotonation entropy of the set of selected reference acids.

for the $A_{3,4}CSH$ and the $HSCA_{3,4}$ systems are shown in Figure 1. Apparently the acidity of A_3CSH is stronger than that of $BrCH_2CO_2H$ but weaker than that of F_2CHCO_2H, and the acidity of A_4CSH is stronger than that of F_2CHCO_2H, but weaker than that of Cl_2CHCO_2H. Similarly the acidity of $HSCA_3$ is stronger than that of F_2CHCO_2H but slightly weaker than that of Cl_2CHCO_2H, and the acidity of $HSCA_4$ is stronger than that of Br_2CHCO_2H but weaker than that of F_3CCO_2H. These spectra also show that $A_{3,4}CSH$ are weaker acids than $HSCA_{3,4}$ respectively. In other words, the thiol group (SH) is more acidic when the cysteine residue is located at the N-terminus rather than at the C-terminus.

The deprotonation enthalpies of the peptides were determined using the extended Cooks kinetic method. The selections of the references for the four peptides are shown in Table 2. For each peptide, the reference acids were chosen based on the stability of the ion signals for the proton-bound heterodimers and the CID product ions. The stability of the heterodimer ion signals is largely determined by the relative acidities of the two acid components within the dimer. For example, $C_3F_7CO_2H$ is too strong an acid compared to A_3CSH. As a result, the signal of the heterodimer ion, $[C_3F_7CO_2\cdot H\cdot A_3CS]^-$, is too weak and the signal of the CID product ion, A_3CS^-, is not stable and hence not reliable. Therefore, $C_3F_7CO_2H$ was not selected as a reference for A_3CSH. The reference acid F_3CCO_2H was eliminated from the A_4CSH system. Although the signal of the heterodimer, $[F_3CCO_2\cdot H\cdot A_4CS]^-$ was stable, the resulting acidity value had an unusually large uncertainty (the reason for this behavior is currently under investigation). The CID experiments were performed at four collision energies: 1.0, 1.5, 2.0, and 2.5 eV (E_{cm}) under the collision gas pressures of 0.5 mTorr. The ion signals produced at 0.5 eV were not stable, and the data obtained were not used for the kinetic analysis. There are two isotopic peaks for the dimer with $ClCH_2CO_2H$ and $BrCH_2CO_2H$ and three isotopic peaks for the dimers with Cl_2CHCO_2H and Br_2CHCO_2H. The most abundant isotopic peaks were selected as the precursor ions for the CID experiments and should be isotopically pure. Some CID product ions fragment further to yield secondary ions at higher collision energies. The ions of $A_{3,4}CS^-$ and $SCA_{3,4}^-$ often fragment further by losing H_2S. Both $Br_2CHCO_2^-$ and $C_3F_7CO_2^-$ yield secondary ions by losing the CO_2 group. The intensities of the secondary ions were combined with the corresponding primary ions for data analysis.

The natural logarithms of the CID product ion branching ratios of [A_nCS^-]/[A_i^-] and [SCA_n^-]/[A_i^-] are shown in Table 2. The data measured at the same collision energy were plotted against the relative deprotonation enthalpies of the reference acids ($\Delta_{acid}H_i - \Delta_{acid}H_{avg}$), eq 2. The plots are shown in Figure 2. Linear regression with the least-squares fit of the data points measured at each collision energy gives a straight line with the slope of $1/RT_{eff}$ and the y-intercept of $-[(\Delta_{acid}H - \Delta_{acid}H_{avg})/RT_{eff} - \Delta(\Delta S)/R]$. The values of the resulting slopes and intercepts along with the derived effective temperatures are summarized in Table 3. The values of T_{eff} for A_4CSH have opposite orders to the increase in collision energy. The reason for this unexpected behavior is unclear at this point and is currently under further investigation.

The values of $\Delta_{acid}H$ for the peptides were derived from the second set of the thermokinetic plots. The plots were generated by plotting the values of $[(\Delta_{acid}H - \Delta_{acid}H_{avg})/RT_{eff} - \Delta(\Delta S)/R]$ obtained from the first set of the plots against the corresponding $1/RT_{eff}$. The plots are shown in Figure 2. Linear regression with a least-squares fit of each set of the data gives a straight line with a slope of $\Delta_{acid}H - \Delta_{acid}H_{avg}$ and an intercept of $-\Delta(\Delta S)/R$. The resulting slopes, intercepts, and entropy terms ($\Delta(\Delta S)$) are listed in Table 4. The deprotonation enthalpies ($\Delta_{acid}H$) of the peptides are obtained by combining the slopes and the corresponding values of $\Delta_{acid}H_{avg}$ (Table 2). The results are 332.2 ± 2.0 kcal/mol (A_3CSH), 325.9 ± 2.0 kcal/mol (A_4CSH), 319.3 ± 2.0 kcal/mol ($HSCA_3$), and 319.2 ± 2.3 kcal/mol ($HSCA_4$) (Table 5).

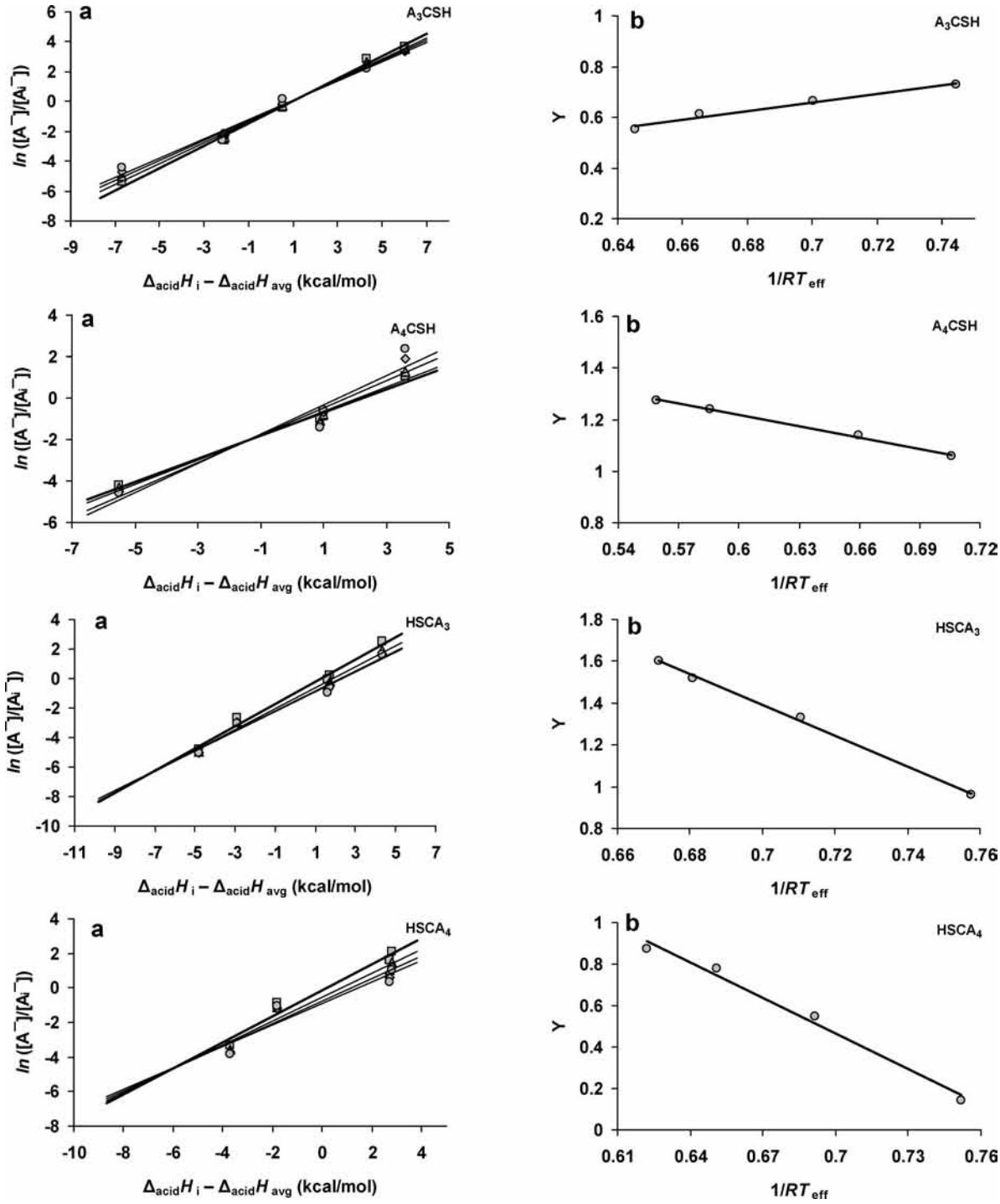

Figure 2. Thermokinetic plots for the four peptide systems, $A_{3,4}CSH$ and $HSCA_{3,4}$, where $[A^-]$ represents $[A_{3,4}CS^-]$ or $[SCA_{3,4}^-]$. The darker line corresponds to the lowest energy data. (a) Plots of $\ln([A^-]/[A_i^-])$ against $\Delta_{acid}H_i - \Delta_{acid}H_{avg}$ from the dissociation of $[A{\cdot}H{\cdot}A_i]^-$ at four collision energies, 1.0 (square), 1.5 (triangle), 2.0 (diamond), and 2.5 (circle) eV (E_{cm}). (b) Plots of $y = (\Delta_{acid}H - \Delta_{acid}H_{avg})/RT_{eff} - \Delta(\Delta S)/R$ against $1/RT_{eff}$.

We evaluated the results obtained from the extended Cooks kinetic method by fitting the experimental data using the ODRFIT program.[52] The resulting values of $\Delta_{acid}H$ are about the same as those obtained from the extended kinetic method, but the uncertainty (Monte Carlo analysis) varies: 332.2 ± 1.2 kcal/mol (A_3CSH), 326.3 ± 1.6 kcal/mol (A_4CSH), 318.6 ± 3.0 kcal/mol ($HSCA_3$), and 317.2 ± 4.0 kcal/mol ($HSCA_4$). The relatively large uncertainties in $HSCA_{3,4}$ are likely due to the fact that the isothermal points of these systems are extrapolated (Figure 2a). We assign the larger uncertainty values from either the kinetic method or the ODRFIT to the measured deprotonation enthalpies (Table 5).

The extended kinetic method is very sensitive to the selection of the reference acids. Ideally, the uncertainty resulting from the reference acid can be minimized by using a large number of references. In practice, a minimum of four references is necessary. It should be pointed out that the uncertainties obtained from the kinetic measurements are relative values. They do not include the absolute error in the overall calibration of the acidity scale of the references.[52]

TABLE 3: Results Obtained from the Linear Regression of the Experimental Data According to Equation 2, Where the Uncertainties Refer to 95% Confidence Level

	A_3CSH[a]			A_4CSH[a]		
E_{cm}, eV	$1/RT_{eff}$	$[(\Delta_{acid}H - \Delta_{acid}H_{avg})/RT_{eff} - \Delta(\Delta S)/R]$	T_{eff}, K	$1/RT_{eff}$	$[(\Delta_{acid}H - \Delta_{acid}H_{avg})/RT_{eff} - \Delta(\Delta S)/R]$	T_{eff}, K
1.0	0.744 ± 0.027	0.728 ± 0.117	676 ± 24	0.559 ± 0.047	1.27 ± 0.16	901 ± 76
1.5	0.700 ± 0.028	0.665 ± 0.119	718 ± 28	0.586 ± 0.062	1.24 ± 0.21	860 ± 91
2.0	0.665 ± 0.031	0.611 ± 0.132	756 ± 35	0.659 ± 0.105	1.14 ± 0.36	763 ± 121
2.5	0.645 ± 0.043	0.553 ± 0.183	779 ± 52	0.706 ± 0.144	1.06 ± 0.49	713 ± 145
	$HSCA_3$[a]			$HSCA_4$[a]		
E_{cm}, eV	$1/RT_{eff}$	$[(\Delta_{acid}H - \Delta_{acid}H_{avg})/RT_{eff} - \Delta(\Delta S)/R]$	T_{eff}, K	$1/RT_{eff}$	$[(\Delta_{acid}H - \Delta_{acid}H_{avg})/RT_{eff} - \Delta(\Delta S)/R]$	T_{eff}, K
1.0	0.757 ± 0.051	0.962 ± 0.169	664 ± 45	0.752 ± 0.101	0.143 ± 0287	669 ± 89
1.5	0.710 ± 0.047	1.329 ± 0.157	708 ± 47	0.691 ± 0.107	0.546 ± 0.303	727 ± 112
2.0	0.681 ± 0.053	1.519 ± 0.176	739 ± 57	0.651 ± 0.126	0.777 ± 0.357	772 ± 149
2.5	0.672 ± 0.063	1.602 ± 0.200	749 ± 71	0.622 ± 0.160	0.872 ± 0.453	809 ± 207

[a] The uncertainties were calculated by weighted orthogonal distance regression (ODR) using the ODRPACK suite of programs.[66]

TABLE 4: Results Obtained from the Second Set of Thermokinetic Plots

peptide	slope	intercept	$\Delta(\Delta S)$(cal/mol K)
A_3CSH	1.779 ± 0.188	-0.586 ± 0.128	1.2 ± 0.2
A_4CSH	-1.478 ± 0.069	2.106 ± 0.045	-4.2 ± 0.2
$HSCA_3$	-7.359 ± 0.223	6.540 ± 0.157	-13.0 ± 0.3
$HSCA_4$	-6.330 ± 0.274	4.910 ± 0.190	-9.7 ± 0.4

TABLE 5: Summary of the Thermochemical Properties Obtained from the Extended Kinetic Method[a]

peptide	$\Delta_{acid}H$	$\Delta_{acid}S$[b]	$\Delta_{acid}G$[c]
A_3CSH	332.2 ± 2.0	24.2 ± 2.0	325.0 ± 2.0
A_4CSH	325.9 ± 2.0	19.0 ± 2.0	320.2 ± 2.0
$HSCA_3$	319.3 ± 3.0	9.9 ± 2.0	316.3 ± 3.0
$HSCA_4$	319.2 ± 4.0	12.8 ± 2.0	315.4 ± 4.0

[a] All values are in kcal/mol. [b] Calculated using the equation $\Delta_{acid}S = \Delta(\Delta S) + \Delta_{acid}S_{avg}$, where $\Delta(\Delta S)$ is the entropy term (Table 4) and $\Delta_{acid}S_{avg}$ is the average deprotonation entropy of the reference acids (Table 2a). [c] Calculated using eq 3, where $T = 298$ K.

The gas-phase acidities ($\Delta_{acid}G$) of the peptides can be derived using eq 3 (where $T = 298$ K) if the deprotonation entropies ($\Delta_{acid}S$) are available. We estimated the deprotonation entropies using the concept of "entropic correction".[76] We calculated $\Delta_{acid}S$ using the relationship $\Delta_{acid}S = \Delta(\Delta S) + \Delta_{acid}S_i$, where $\Delta(\Delta S)$ is obtained from the second set of thermokinetic plots (Table 4) and $\Delta_{acid}S_i$ is estimated as the average of the deprotonation entropies of the reference acids ($\Delta_{acid}S_{avg}$, Table 2). The resulting $\Delta_{acid}S$ values for the four peptides are summarized in Table 5. An average of ± 2 cal/mol K is assigned as the uncertainty for these values. Combining the values of $\Delta_{acid}H$ and $\Delta_{acid}S$, we obtained $\Delta_{acid}G$ for the peptides, and the results are summarized in Table 5. We assigned the same uncertainties as those for $\Delta_{acid}H$.

Results of Computational Studies

Simulated annealing yielded a pool of low energy conformations. For both the $A_{3,4}CSH$ and the $HSCA_{3,4}$ series, the conformations of the neutral peptides are similar and mainly existed as random coils, while the conformations of the deprotonated peptides are significantly different between the two series. The $A_{3,4}CS^-$ series existed as random coils with the negatively charged sulfide atom solvated by the nearby N−H groups through hydrogen bonding or charge−dipole interaction. The $^-SCA_{3,4}$ series existed in partial helical loops with the sulfide anion pointing to the axis of the helix. Representative conformations of the deprotonated peptides are shown in Figure 3.

We also examined the possible conformations of the proton-bound dimers of $[Br_2CHCO_2 \cdot H \cdot A_4CS]^-$ and $[Br_2CHCO_2 \cdot H \cdot SCA_4]^-$ by performing geometry optimizations at the AM1 level. In this case, a single starting geometry was used for each dimer. For both dimers, the initial geometry has a helical conformation within the peptide part. In the optimized conformation, the peptide portion in $[Br_2CHCO_2 \cdot H \cdot A_4CS]^-$ becomes a random coil, while the peptide portion in $[Br_2CHCO_2 \cdot H \cdot SCA_4]^-$ remains a helix (Figure 3).

The theoretical deprotonation enthalpies ($\Delta_{acid}H$(calc)) were calculated using the B3LYP/6-31+G(d)//AM1 procedure. For each peptide species, five out of the ten low energy conformations were chosen for deriving the theoretical acidities. The enthalpy (at 298 K) corresponding to each conformation was calculated by combining the electronic energy (B3LYP/6-31+G(d)) and the zero-point energy plus the thermal correction calculated at the AM1 level. For each peptide species, the lowest value of the enthalpy is chosen and is listed in Table 6. The enthalpies of the reference acid (ethanethiol) are also shown in Table 6. The theoretical deprotonation enthalpy for each peptide was derived using the isodesmic proton transfer reaction with ethanethiol ($\Delta_{acid}H = 355.7$ kcal/mol[45]) as the reference acid (eq 4). The results are summarized in Table 6. These theoretical values agree well with the experimental results (Table 5).

We evaluated the computational method as well by comparing the result obtained from the B3LYP//AM1 procedure to that obtained from the B3LYP//B3LYP procedure using the $HSCA_3$ system. We selected the lowest energy conformations obtained from the AM1 procedure as the input geometry. The input geometry was further optimized at the B3LYP/6-31+G(d) level followed by frequency calculations at the same level of theory. The resulting theoretical deprotonation enthalpy (319.3 kcal/mol) is about the same as that (320.6 kcal/mol) calculated using the B3LYP/6-31+G(d)//AM1 procedure. The B3LYP//AM1 procedure is less expensive and is used for this research.

Discussion

The CID bracketing experiments yielded the relative acidities of the four peptides, $A_{3,4}CSH$ and $HSCA_{3,4}$. The two N-terminal cysteine peptides, $HSCA_{3,4}$, are clearly more acidic than the two C-terminal cysteine peptides, $A_{3,4}CSH$. For the same type of

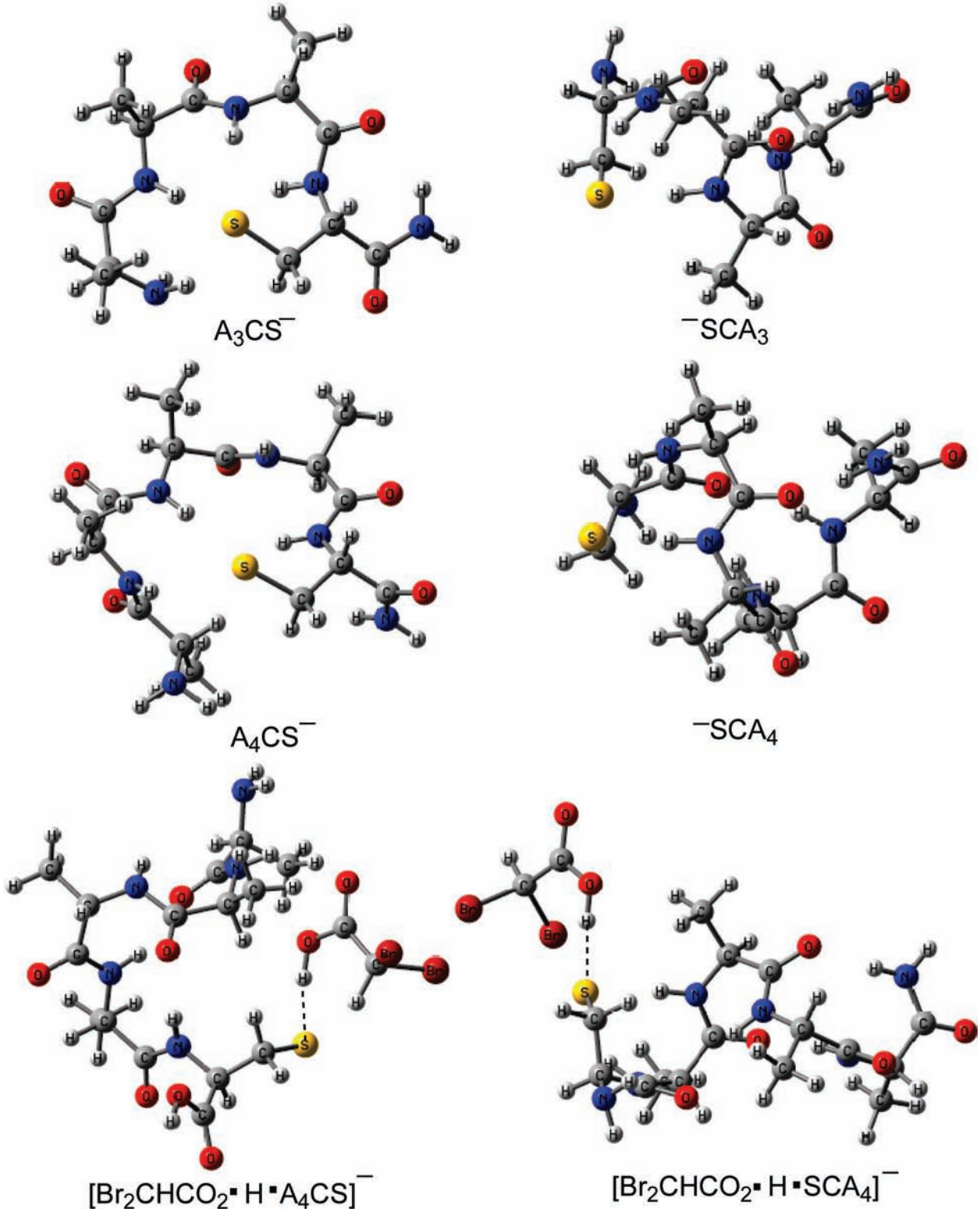

Figure 3. Conformations for the deprotonated peptides, A_3CS^-, A_4CS^-, $^-SCA_3$, and $^-SCA_4$, obtained from the AM1//simulated annealing procedure and the conformations of the heterodimer ions, $[A_4CS \cdot H \cdot Cl_2CHCO_2]^-$ and $[SCA_4 \cdot H \cdot Cl_2CHCO_2]^-$, obtained at the AM1 level.

peptides, the longer one is more acidic than the shorter one. The extended kinetic method yielded the deprotonation enthalpies ($\Delta_{acid}H$) and the approximate values of deprotonation entropies ($\Delta_{acid}S$). The gas-phase acidities ($\Delta_{acid}G$) of the peptides were derived by combining the values of $\Delta_{acid}H$ and $\Delta_{acid}S$. The acidity of $HSCA_3$ is about 10 kcal/mol stronger than that of A_3CSH, and the acidity of $HSCA_4$ is about 5 kcal/mol stronger than that of A_4CSH. Computational studies show distinctly different conformations of the two series of deprotonated peptides. Theoretically predicted deprotonation enthalpies agree reasonably well with the experimental results.

Conformational Effects on the Acidity. The experiments strongly suggest that the cysteine residue is more acidic when it is placed at the N-terminus than at the C-terminus. This implies that the N-terminal thiolate anion (S^-) is stabilized more than the C-terminal one. Computational studies show that the

TABLE 6: Computational Results for the Peptides $A_{3,4}CSH$ and $HSCA_{3,4}$

peptide	H(AH) (hartree)	$H(A^-)$ (hartree)	$\Delta_{acid}H$ (kcal/mol)
A_3CSH	−1443.672592	−1443.14566	334.2
A_4CSH	−1690.915159	−1690.398620	327.7
$HSCA_3$	−1443.666847	−1443.16172	320.6
HSCA4	−1690.910694	−1690.408757	318.6
CH_3CH_2SH	−477.936176	−477.378935	355.7 ± 2.1 (expt)[a]

[a] Literature experimental value.[45]

deprotonated C-cysteine peptides, $A_{3,4}CS^-$, are in random coils, and the negatively charged thiolate group (S^-) is largely stabilized by hydrogen-bonding interactions with nearby NH groups. On the other hand, the deprotonated N-cysteine peptides, $^-SCA_{3,4}$, exist in partial helices with the thiolate anion pointing to the axis of the helix loop. In the latter case, the thiolate anion may largely be stabilized by the interaction with the helix macrodipole in addition to the possible hydrogen-bonding interactions. The helix macrodipole is an intrinsic property of helical peptides, arising from the alignment of the polar peptide bonds, which in turn creates a dipolar electrostatic field with a partial positive charge at the N-terminus and a partial negative charge at the C-terminus. Apparently, the helix macrodipole has a stronger stabilization effect toward the thiolate anion than that of the hydrogen-bonding interaction. This possibility will be tested using longer peptides for which the helical conformations will be more stable (work in progress).

Entropy Effects on the Acidity. The term $\Delta(\Delta S)$ corresponds to the differences in the activation entropies between the two dissociation channels, the formation of the deprotonated peptide ($\Delta S^{\ddagger}$) and the formation of the deprotonated reference acid ($\Delta S^{\ddagger}_i$), $\Delta(\Delta S) = \Delta S^{\ddagger} - \Delta S^{\ddagger}_i$. If the reverse activation barriers are negligibly small, then the entropy term can be considered as the difference in the deprotonation entropies between the peptide and the reference acid, $\Delta(\Delta S) = \Delta_{acid}S - \Delta_{acid}S_i$. One important condition for the validity of the extended kinetic method is the assumption that $\Delta(\Delta S)$ is about constant for all the reference acids and at all temperatures. This is expected to be achieved by using reference acids with similar structures.[48,53] In this work, the reference acids are halogenated carboxylic acids, and small geometrical changes are expected upon deprotonation. This means that the reference acids would contribute negligible or very small entropy change for $\Delta(\Delta S)$.

Considering the size differences between the peptides and the references acids, the entropy terms in the $A_{3,4}CSH$ systems are surprisingly small (∼1−4 cal/mol K, Table 4). Computational studies show that $A_{3,4}CS^-$ exist in random coils with extensive intramolecular hydrogen-bonding interactions. One would expect significant decreases in structural flexibility upon deprotonation, and as a consequence, the deprotonation entropies for these peptides would be small. However, opposite results were observed. The estimated deprotonation entropies of these two peptides are around 19−24 cal/mol K (Table 5), which are close to those of the reference acids. There must be some factor(s) that overcome this negative entropy effect. The first explanation might be the conformational effect. The peptide already forms a highly ordered coil in the proton-bound dimer through internal solvation of the partial negative charge. This coil remains intact upon dissociation of the proton-bound dimer ion. The coillike conformation is clearly seen in the computed structure of $[Br_2CHCO_2 \cdot H \cdot A_4CS]^-$ (Figure 3, although the structure of the dimer was calculated based on a single starting geometry, the optimized structure is likely the low energy one). The second explanation might be the entropy of mixing. Although the individual deprotonated peptide is highly ordered because of extensive hydrogen bonding, there are many possible structures corresponding to the internally solvated peptide. In other words, the deprotonated peptide presumably has as many conformations as that of the neutral peptide. Indeed, computational studies suggested numerous random conformations of $A_{3,4}CS^-$ having similar energies.

On the other hand, the entropy terms for the $HSCA_{3,4}$ systems are large and negative (∼ −10 to −13 cal/mol K). The estimated deprotonation entropies are relatively small (∼10−13 cal/mol K). The negative entropy effect indicates an increase in rigidity of the peptides upon deprotonation. This might be a consequence of the formation of the highly ordered helical conformation. As shown in the computed structures of $[Br_2CHCO_2 \cdot H \cdot SCA_4]^-$ and $^-SCA_4$ (Figure 3), the $^-SCA_4$ portion remains a ridged helix throughout the dissociation of $[Br_2CHCO_2 \cdot H \cdot SCA_4]^-$. When closely examining these structures, one can see that the isolated $^-SCA_4$ is more compact than the one in the dimer as well as the neutral peptide (data not shown). This means that the entropy change for the formation of $^-SCA_4 + Br_2CHCO_2H$ is less favored than that for the formation of $HSCA_4 + Br_2CHCO_2^-$.

Conclusions

We have determined the gas-phase deprotonation enthalpies of four cysteine-polyalanine peptides, $A_{3,4}CSH$ and $HSCA_{3,4}$, using the extended Cooks kinetic method with full entropy analysis. The values obtained are $\Delta_{acid}H(A_3CSH) = 332.2 \pm 2.0$ kcal/mol, $\Delta_{acid}H(A_4CSH) = 325.9 \pm 2.0$ kcal/mol, $\Delta_{acid}H(HSCA_3) = 319.3 \pm 3.0$ kcal/mol, and $\Delta_{acid}H(HSCA_4) = 319.2 \pm 4.0$ kcal/mol. Theoretically (B3LYP/6-31+G(d)//AM1) predicted deprotonation enthalpies, 334.2 kcal/mol (A_3CSH), 327.7 kcal/mol (A_4CSH), 320.6 kcal/mol ($HSCA_3$), and 318.6 kcal/mol ($HSCA_4$), are in good agreement with the experiments. The estimated deprotonation entropies ($\Delta_{acid}S$) for the $A_{3,4}CSH$ systems are relatively large (∼19−24 cal/mol K), while for the $HSCA_{3,4}$ systems they are relatively small (∼10−13 cal/mol K). The resulting gas-phase acidities ($\Delta_{acid}G$) are 325.0 ± 2.0 kcal/mol (A_3CSH), 320.2 ± 2.0 kcal/mol (A_4CSH), 316.3 ± 3.0 kcal/mol ($HSCA_3$), and 315.4 ± 4.0 kcal/mol ($HSCA_4$).

The two N-terminal cysteine peptides, $HSCA_{3,4}$, are significantly more acidic than the corresponding C-terminal ones, $A_{3,4}CSH$. $HSCA_3$ is a stronger acid than A_3CSH by about 10 kcal/mol, and $HSCA_4$ is a stronger acid than A_4CSH by about 5 kcal/mol. The high acidities of the former are likely due to the helical conformational effects for which the thiolate anion may be strongly stabilized by the interaction with the helix macrodipole. It is expected that the macrodipolar effect is significant for a peptide with a stable helical conformation. As a result, the effective acidity of an acidic amino acid residue will be different depending on the location of the residue in a peptide and protein.

Acknowledgment. This research was supported by The American Chemical Society Petroleum Research Fund Type-G Grant and the National Science Foundation (CHE-0749737). The instrument usage was provided by the Mass Spectrometry Facility at the University of the Pacific. We thank Professors K. Ervin and P. Armentrout for allowing the use of their ODRFIT program.

References and Notes

(1) Honig, B.; Nicholls, A. *Science* **1995**, *268*, 1144–1149.
(2) Fersht, A. *Structure and mechanism in protein science*; W.H. Freeman & Co.: New York, 1999.

(3) Forsyth, W. R.; Antosiewicz, J. M.; Robertson, A. D. *Proteins: Struct., Funct., Genet.* **2002**, *48*, 388–403.
(4) Huyghues-Despointes, B. M. P.; Scholtz, J. M.; Baldwin, R. L. *Protein Sci.* **1993**, *2*, 1604–1611.
(5) Martin, J. L. *Structure* **1995**, *3*, 245–250.
(6) Carvalho, A. P.; Fernandes, P. A.; Ramos, M. J. *Prog. Biophys. Mol. Biol.* **2006**, *91*, 229–248.
(7) Carvalho, A. T. P.; Swart, M.; van Stralen, J. N. P.; Fernandes, P. A.; Ramos, M. J.; Bickelhaupt, F. M. *J. Phys. Chem. B* **2008**, *112*, 2511–2523.
(8) Takahashi, N.; Creighton, T. E. *Biochemistry* **1996**, *35*, 8342–8353.
(9) Gan, Z. R.; Sardana, M. K.; Jacobs, J. W.; Polokoff, M. A. *Arch. Biochem. Biophys.* **1990**, *282*, 110–115.
(10) Philipps, B.; Glockshuber, R. *J. Biol. Chem.* **2002**, *277*, 43050–43057.
(11) Miranda, J. J. L. *Protein Sci.* **2003**, *12*, 73–81.
(12) Hol, W. G.; van Duijnen, P. T.; Berendsen, H. J. *Nature* **1978**, *273*, 443–446.
(13) Shoemaker, K. R.; Kim, P. S.; York, E. J.; Stewart, J. M.; Baldwin, R. L. *Nature* **1987**, *326*, 563–567.
(14) Joshi, H. V.; Meier, M. S. *J. Am. Chem. Soc.* **1996**, *118*, 12038–12044.
(15) Kortemme, T.; Creighton, T. E. *J. Mol. Biol.* **1995**, *253*, 799–812.
(16) Gallo, E. A.; Gellman, S. H. *J. Am. Chem. Soc.* **1994**, *116*, 11560–11561.
(17) Warshel, A. *Acc. Chem. Res.* **1981**, *14*, 284–290.
(18) Nishikaze, T.; Takayama, M. *Int. J. Mass Spectrom.* **2007**, *268*, 47–59.
(19) Qin, J.; Chait, B. T. *J. Am. Chem. Soc.* **1995**, *117*, 5411–5412.
(20) Gu, C.; Tsaprailis, G.; Breci, L.; Wysocki, V. H. *Anal. Chem.* **2000**, *72*, 5804–5813.
(21) Huang, Y.; Wysocki, V. H.; Tabb, D. L.; Yates, J. R. *Int. J. Mass Spectrom.* **2002**, *219*, 233–244.
(22) Tsaprailis, G.; Somogyi, A.; Nikolaev, E. N.; Wysocki, V. H. *Int. J. Mass Spectrom.* **2000**, *195/196*, 467–479.
(23) Lioe, H.; Laskin, J.; Reid, G. E.; O'Hair, R. A. J. *J. Phys. Chem. A* **2007**, *111*, 10580–10588.
(24) Bowie, J. H.; Brinkworth, C. S.; Dua, S. *Mass Spectrom. Rev.* **2002**, *21*, 87–107.
(25) Ewing, N. P.; Cassady, C. J. *J. Am. Soc. Mass Spectrom.* **2001**, *12*, 105–116.
(26) Harrison, A. G.; Young, A. B. *Int. J. Mass Spectrom.* **2006**, *255*−*256*, 111–122.
(27) Bilusich, D.; Brinkworth, C. S.; Bowie, J. H. *Rapid Commun. Mass Spectrom.* **2004**, *18*, 544–552.
(28) Lee, S.-W.; Kim, H. S.; Beauchamp, J. L. *J. Am. Chem. Soc.* **1998**, *120*, 3188–3195.
(29) Boutin, M.; Bich, C.; Afonso, C.; Fournier, F.; Tabet, J.-C. *J. Mass Spectrom.* **2007**, *42*, 25–35.
(30) Ewing, N. P.; Cassady, C. J. *J. Am. Soc. Mass Spectrom.* **1999**, *10*, 928–940.
(31) Jurchen, J. C.; Cooper, R. E.; Williams, E. R. *Int. J. Mass Spectrom.* **2003**, *14*, 1477–1487.
(32) Caldwell, G. W.; Renneboog, R.; Kebarle, P. *Can. J. Chem.* **1989**, *67*, 611–618.
(33) Locke, M. J.; McIver, R. T., Jr. *Int. J. Mass Spectrom.* **1983**, *105*, 4226–4232.
(34) Meot-Ner, M.; Hunter, E. P.; Field, F. H. *J. Am. Chem. Soc.* **1979**, *101*, 686–689.
(35) Jones, C. M.; Bernier, M.; Carson, E.; Colyer, K. E.; Metz, R.; Pawlow, A.; Wischow, E. D.; Webb, I.; Andriole, E. J.; Poutsma, J. C. *Int. J. Mass Spectrom.* **2007**, *267*, 54–62.
(36) Tian, Z.; Pawlow, A.; Poutsma, J. C.; Kass, S. R. *J. Am. Chem. Soc.* **2007**, *129*, 5403–5407.
(37) Li, Z.; Matus, M. H.; Velazquez, H. A.; Dixon, D. A.; Cassady, C. J. *Int. J. Mass Spectrom.* **2007**, *265*, 213–223.
(38) O'Hair, R. A. J.; Bowie, J. H.; Gronert, S. *Int. J. Mass Spectrom. Ion Processes* **1992**, *117*, 23–36.
(39) Fournier, F.; Afonso, C.; Fagin, A. E.; Gronert, S.; Tabet, J.-C. *J. Am. Soc. Mass Spectrom.* **2008**, *19*, 1887–1896.
(40) Jia, B.; Angel, L. A.; Ervin, K. M. *J. Phys. Chem. A* **2008**, *112*, 1773–1782.
(41) Woo, H.-K.; Lau, K.-C.; Wang, X.-B.; Wang, L.-S. *J. Phys. Chem. A* **2006**, *110*, 12603–12606.
(42) Oomens, J.; Steill, J. D.; Redlich, B. *J. Am. Chem. Soc.* **2009**, *131*, 4310–4319.
(43) Carr, S. R.; Cassady, C. J. *J. Mass Spectrom.* **1997**, *32*, 959–967.
(44) Tan, J. P.; Ren, J. *J. Am. Soc. Mass Spectrom.* **2007**, *18*, 188–194.
(45) *NIST Chemistry Webbook*, NIST Standard Reference Database Number 69; Linstrom, P. J., Mallard, W. G., Eds.; National Institute of Standards and Technology: Gaithersburg MD, 20899(http://webbook.nist.gov).
(46) Cooks, R. G.; Patrick, J. S.; Kotiaho, T.; McLuckey, S. A. *Mass Spectrom. Rev.* **1994**, *13*, 287–339.
(47) Cooks, R. G.; Koskinen, J. T.; Thomas, P. D. *J. Mass Spectrom.* **1999**, *34*, 85–92.
(48) Cheng, X.; Wu, Z.; Fenselau, C. *J. Am. Chem. Soc.* **1993**, *115*, 4844–4848.
(49) Cerda, B. A.; Wesdemiotis, C. *J. Am. Chem. Soc.* **1996**, *118*, 11884–11892.
(50) Cooks, R. G.; Wong, P. S. H. *Acc. Chem. Res.* **1998**, *31*, 379–386.
(51) Williams, T. I.; Denault, J. W.; Cooks, R. G. *Int. J. Mass Spectrom.* **2001**, *210/211*, 133–146.
(52) Ervin, K. M.; Armentrout, P. B. *J. Mass Spectrom.* **2004**, *39*, 1004–1015.
(53) Drahos, L.; Peltz, C.; Vekey, K. *J. Mass Spectrom.* **2004**, *39*, 1016–1024.
(54) Bouchoux, G. *J. Phys. Chem. A* **2006**, *110*, 8259–8265.
(55) Bouchoux, G.; Sablier, M.; Berruyer-Penaud, F. *J. Mass Spectrom.* **2004**, *39*, 986–997.
(56) Wesdemiotis, C. *J. Mass Spectrom.* **2004**, *39*, 998–1003.
(57) Bouchoux, G. *J. Mass Spectrom.* **2006**, *41*, 1006–1013.
(58) Harrison, A. G. *Mass Spectrom. Rev.* **1997**, *16*, 201–217.
(59) Drahos, L.; Vekey, K. *J. Mass Spectrom.* **1999**, *34*, 79–84.
(60) Armentrout, P. B. *J. Mass Spectrom.* **1999**, *34*, 74–78.
(61) Laskin, J.; Futrell, J. H. *J. Phys. Chem. A* **2000**, *104*, 8829–8837.
(62) Ervin, K. M. *J. Am. Soc. Mass Spectrom.* **2002**, *13*, 435–452.
(63) Norrman, K.; McMahon, T. B. *Int. J. Mass Spectrom.* **1998**, *176*, 87–97.
(64) Meot-Ner, M.; Somogyi, A. *Int. J. Mass Spectrom.* **2007**, *267*, 346–356.
(65) Armentrout, P. B. *J. Am. Soc. Mass Spectrom.* **2000**, *11*, 371–379.
(66) Boggs, P. T.; Byrd, R. H.; Rogers, J. E.; Schnabel, R. B. *Report NISTIR 92-4834*; National Institute of Standards and Technology: Gaithersburg, MD, 1992.
(67) Gutte, B., Ed. *Peptides: Synthesis, Structures, and Applications*, Academic; San Diego, 1995.
(68) Barany, G.; Merrifield, R. B. *Peptides (N. Y., 1979*−*1987)* **1980**, *2*, 1–284.
(69) Chan, W. C.; White, P. D., Eds. *Fmoc Solid Phase Peptide Synthesis: A Practical Approach*, Oxford Univ Press: Oxford **2000**.
(70) Dewar, M. J. S.; Zoebisch, E. G.; Healy, E. F.; Stewart, J. J. P. *J. Am. Chem. Soc.* **1985**, *107*, 3902–3909.
(71) Frisch, M. J.; Trucks, G. W.; Schlegel, H. B.; Scuseria, G. E.; Robb, M. A.; Cheeseman, J. R.; Montgomery, J. A., Jr.; Vreven, T.; Kudin, K. N.; Burant, J. C.; Millam, J. M.; Iyengar, S. S.; Tomasi, J.; Barone, V.; Mennucci, B.; Cossi, M.; Scalmani, G.; Rega, N.; Petersson, G. A.; Nakatsuji, H.; Hada, M.; Ehara, M.; Toyota, K.; Fukuda, R.; Hasegawa, J.; Ishida, M.; Nakajima, T.; Honda, Y.; Kitao, O.; Nakai, H.; Klene, M.; Li, X.; Knox, J. E.; Hratchian, H. P.; Cross, J. B.; Bakken, V.; Adamo, C.; Jaramillo, J.; Gomperts, R.; Stratmann, R. E.; Yazyev, O.; Austin, A. J.; Cammi, R.; Pomelli, C.; Ochterski, J. W.; Ayala, P. Y.; Morokuma, K.; Voth, G. A.; Salvador, P.; Dannenberg, J. J.; Zakrzewski, V. G.; Dapprich, S.; Daniels, A. D.; Strain, M. C.; Farkas, O.; Malick, D. K.; Rabuck, A. D.; Raghavachari, K.; Foresman, J. B.; Ortiz, J. V.; Cui, Q.; Baboul, A. G.; Clifford, S.; Cioslowski, J.; Stefanov, B. B.; Liu, G.; Liashenko, A.; Piskorz, P.; Komaromi, I.; Martin, R. L.; Fox, D. J.; Keith, T.; Al.Laham, M. A.; Peng, C. Y.; Nanayakkara, A.; Challacombe, M.; Gill, P. M. W.; Johnson, B.; Chen, W.; Wong, M. W.; Gonzalez, C.; Pople, J. A. *Gaussian 03*, revision A.1.; Gaussian, Inc.: Wallingford CT, 2004..
(72) Parr, R. G.; Yang, W. *Density-functional Theory of Atoms and Molecules*; Clarendon Press: New York, 1989.
(73) Becke, A. D. *Phys. Rev. A* **1988**, *38*, 3098–3100.
(74) Becke, A. D. *J. Chem. Phys.* **1993**, *98*, 5648–5652.
(75) Lee, C.; Yang, W.; Parr, R. G. *Phys. Rev. B* **1988**, *37*, 785–789.
(76) Zheng, X.; Cooks, R. G. *J. Phys. Chem. A* **2002**, *106*, 9939–9946.

JP903594A